Acta Oceanol. Sin., 2014, Vol. 33, No. 1, P. 64–76
DOI: 10.1007/s13131-014-0425-6
http://www.hyxb.org.cn
E-mail: hyxbe@263.net

How does the Indian Ocean subtropical dipole trigger the tropical Indian Ocean dipole via the Mascarene high?

FENG Junqiao[1,2*], HU Dunxin[1,2], YU Lejiang[3]

[1] Institute of Oceanology, Chinese Academy of Sciences, Qingdao 266071, China
[2] Key Laboratory of Ocean Circulation and Wave, Chinese Academy of Sciences, Qingdao 266071, China
[3] Applied Hydrometeorological Research Institute, Nanjing University of Information Science and Technology, Nanjing 210044, China

Received 13 June 2012; accepted 24 December 2013

Abstract
The variation in the Indian Ocean is investigated using Hadley center sea surface temperature (SST) data during the period 1958–2010. All the first empirical orthogonal function (EOF) modes of the SST anomalies (SSTA) in different domains represent the basin-wide warming and are closely related to the Pacific El Niño–Southern Oscillation (ENSO) phenomenon. Further examination suggests that the impact of ENSO on the tropical Indian Ocean is stronger than that on the southern Indian Ocean. The second EOF modes in different domains show different features. It shows a clear east-west SSTA dipole pattern in the tropical Indian Ocean (Indian Ocean dipole, IOD), and a southwest-northeast SSTA dipole in the southern Indian Ocean (Indian Ocean subtropical dipole, IOSD). It is further revealed that the IOSD is also the main structure of the second EOF mode on the whole basin-scale, in which the IOD pattern does not appear. A correlation analysis indicates that an IOSD event observed during the austral summer is highly correlated to the IOD event peaking about 9 months later. One of the possible physical mechanisms underlying this highly significant statistical relationship is proposed. The IOSD and the IOD can occur in sequence with the help of the Mascarene high. The SSTA in the southwestern Indian Ocean persists for several seasons after the mature phase of the IOSD event, likely due to the positive wind–evaporation–SST feedback mechanism. The Mascarene high will be weakened or intensified by this SSTA, which can affect the atmosphere in the tropical region by teleconnection. The pressure gradient between the Mascarene high and the monsoon trough in the tropical Indian Ocean increases (decreases). Hence, an anticyclone (cyclone) circulation appears over the Arabian Sea-India continent. The easterly or westerly anomalies appear in the equatorial Indian Ocean, inducing the onset stage of the IOD. This study shows that the SSTA associated with the IOSD can lead to the onset of IOD with the aid of atmosphere circulation and also explains why some IOD events in the tropical tend to be followed by IOSD in the southern Indian Ocean.

Key words: Indian Ocean dipole, Indian Ocean subtropical dipole, Mascarene high

Citation: Feng Junqiao, Hu Dunxin, Yu Lejiang. 2014. How does the Indian Ocean subtropical dipole trigger the tropical Indian Ocean dipole via the Mascarene high? Acta Oceanologica Sinica, 33(1): 64–76, doi: 10.1007/s13131-014-0425-6

1 Introduction

The Indian Ocean is the smallest of all oceans. It has been previously considered as a passive element in the tropical system, essentially controlled by El Niño through an atmospheric bridge (Klein et al., 1999; Lau and Nath, 2000, 2003; Alexander et al., 2002), and by the Asian summer monsoon via air-sea fluxes associated with the monsoon flow (Webster et al., 1998). However, in recent times, a great number of the studies have documented Indian Ocean variability as an important driving factor in the low-frequency variations of the climate, contrasting with the classical view (e.g., Wang et al., 1999; Wang et al., 2004; Wu et al., 2009, 2011; Zhou et al., 2009; Wu et al., 2010; Subrahmanyam and Wang, 2011). In particular, air-sea interactions in the tropical Indian Ocean have been extensively explored after Saji et al. (1999) proposing the concept of the tropical Indian Ocean dipole (IOD), which is characterized by opposite signs of sea surface temperature anomalies (SSTA) in the western tropical Indian Ocean and that in the eastern tropical Indian Ocean. It is strongly connected with the precipitation anomalies in the eastern Africa and Indonesia. Among the various issues, the mechanism of IOD occurrence is the most important. Several mechanisms have been proposed to explain the formation of IOD.

First, one important mechanism that plays a fundamental role in the formation of IOD is the Bjerknes feedback (Bjerknes, 1969), which is induced by an equatorial easterly wind (e.g., Saji et al., 1999; Li et al., 2003; Fischer et al., 2005). Second, a wind-evaporation-SST feedback in the southeastern tropical Indian Ocean is considered as another air-sea coupled process that favours the growth of IOD (Hilary et al., 2005). The southeasterly wind along Sumatra can lead to the ocean-to-atmosphere latent heat flux by increasing the evaporation on the one hand (Baquero-Bernal et al., 2002; Li et al., 2003), and inducing the upwelling on the other hand. As a result, the SST cools down

Foundation item: The National Natural Science Foundation of China under contract Nos 41106016 and 41330963; the National Basic Research Program (973 Program) of China under contract No. 2012CB417403.
*Corresponding author, E-mail: fengjunqiao@qdio.ac.cn

there. Third, some previous studies also show that Rossby and Kelvin wave propagation is an important oceanic dynamic process during the IOD event (e.g., Webster et al., 1999; Rao et al., 2002; Xie et al., 2002; Feng and Meyers, 2003). In addition, as a key element connecting the Pacific and Indian Oceans in the tropics, the Indonesian throughflow (ITF) is a critical part of the "global conveyor belt" (Gordon, 1986; Liu et al., 2005; Liu et al., 2010; Liu et al., 2012). Its variation has also been proposed as a forcing factor of the IOD event. Since the weakening of it results in the cooling of SSTA in the southeastern tropical Indian Ocean, it becomes a trigger of IOD (e.g., Annamalai et al., 2003; Cai et al., 2005). However, the details of the formation and variation of the IOD are not completely understood. Physical processes in different IOD events are not the same.

On the study of the formation mechanism of IOD, researchers have been focusing on the debate of whether the IOD is forced by El Niño Southern Oscillation (ENSO) or by the interior Indian Ocean coupled process. Some authors argue that IOD events are triggered by the ENSO (e.g., Baquero-Bernal et al., 2002; Hendon, 2003; Shinoda et al., 2004), in which Walker circulation is the connecting bridge (e.g., Latif and Barnett, 1995; Klein et al., 1999; Lau and Nath, 2000). It is only the stochastic forcing of the atmosphere, not necessarily related to the ocean dynamics (Baquero-Bernal et al., 2002). Nevertheless, others claim that the IOD is the manifestation of coupled ocean-atmosphere instability inherent to the Indian Ocean-monsoon system, which is independent of the ENSO (e.g., Saji et al., 1999; Ashok et al., 2003; Behera et al., 2006). The propagation of Rossby and Kelvin waves, which affects the thermocline variability, is self-maintaining in the Indian Ocean air-sea coupled system (Webster et al., 1999).

Recently, more and more numerical experiment results suggest that the IOD event can be forced by the ENSO and the air-sea coupled variability in the interior Indian Ocean (e.g., Yu and Lau, 2004; Fischer et al., 2005; Feng and Bai, 2010). The study results of Fischer et al. (2005) and Zhao et al. (2009) indicate that the interior variability triggering the IOD originates from Mascarene high in the southern Indian Ocean. Hastenrath and Polzin (2004) also suggest that the equatorial easterly/westerly wind, which plays a key role in the IOD evolution, is highly related to the Mascarene high and monsoon wind in the southern Indian Ocean. More recently, another SST dipole mode in the southern Indian Ocean, an Indian Ocean subtropical dipole (IOSD), with mature phase locked to the austral summer, has also been documented by Behera and Yamagata (2001). Such subtropical events are related to Mascarene high (e.g., Venegas et al., 1998; Goddard and Graham, 1999; Behera and Yamagata, 2001; Reason, 2001, 2002), which is not associated with extreme phases of the ENSO (Behera and Yamagata, 2001; Jia and Li, 2005; Terray and Dominiak, 2005). While the tropical and subtropical SST dipoles are proposed, their relationship and associated physical processes have been much less studied. Some authors argue that the IOSD may be another important trigger of the IOD (Fischer et al., 2005; Liu and Yu, 2006; Terray et al., 2007). When IOSD leads IOD for about 9 months, they are highly positive correlated (Liu and Yu, 2006). By carrying out numerical experiments, Fischer et al. (2005) and Terray et al. (2007) pointed out that the SSTA in the eastern pole of the IOSD produced in the later austral summer may be a significant precursor of the IOD event occurring several months later. However, in their study, only the role of SSTA in the eastern pole of the IOSD is emphasized. Moreover, not all of SSTA in the eastern pole of the IOSD is completely related to the IOSD. In fact, the role of SSTA in the western pole of the IOSD underlying the Mascarene high is also important during the evolution of IOSD. It should be granted more attention in considering the role of IOSD in triggering the IOD.

In this study, we examine the force-and-response relationship between SST variations in the south Indian Ocean and the tropical Indian Ocean associated with the two dipoles. The primary goal of this study is to further investigate the role of IOSD in triggering the IOD event.

The rest of the paper is organized as follows. Section 2 describes data and methods. Section 3 presents the interannual variability of the SST in the Indian Ocean by empirical orthogonal function (EOF) analysis. The two dipole modes of the Indian Ocean are described in this section. Then, in Section 4, a possible relationship between IOSD and IOD is found via lead-lag correlation analysis. After that, in order to document the role of the subtropical Indian Ocean SSTA in the evolution of IOD, we will examine the atmospheric field associated with the SST variability using the lead-lag correlation analysis. In addition, the composite SST evolution during a nearly 1 a period associated with the IOSD event, which is followed by the IOD event, will also be investigated. Finally, we summarize our results in Section 5.

2 Data and methods

Monthly atmospheric circulation data for the period 1958–2001 and 2002–2010 are obtained from the European Centre for Medium-Range Weather Forecasts (ECMWF) 40 a reanalysis (ERA-40) and ECMWF interim reanalysis (ERA-Interim) products, respectively. The ERA-interim is the latest ECMWF global atmospheric reanalysis of the period 1979 to present. The resolution of ERA-40 is 2.5° by 2.5°, whereas 1.5° by 1.5° for the ERA-Interim. In order to construct the long time series from 1958 to 2010 by the combination of the ERA-40 and the ERA-interim, the ERA-interim data sets are interpolated into a 2.5° by 2.5° latitude-longitude grid. The atmosphere fields include a sea level pressure (SLP), 850 hPa winds, 200 hPa winds, and 500 hPa vertical velocities (omega). The heat flux data from the National Center for Environmental Prediction/National Center for Atmospheric Research (NCEP/NCAR) reanalysis I is also used. A detailed description of the data assimilation system that produces this data set is given by Kalnay et al. (1996). It is with a spatial resolution of 2.5° by 2.5° for the period 1958–2010. Monthly SST data from 1958 to 2010 are extracted from the UK Met Office Hadley Centre's sea ice and SST data sets (HadISST1). The resolution is 1° latitude by 1° longitude. The climatology of the above data sets are calculated for each calendar month at each grid point by averaging the data over 1958–2010. Monthly anomalies are defined as deviations from the mean annual cycle.

In this paper, in order to appropriately describe the characteristics of the IOSD and IOD mode, signals of interannual variability in different regions of the Indian Ocean will be extracted from the monthly SSTA, by carrying out the EOF analysis. In addition, the lead-lag correlation is employed to illustrate the potential causal relationship between two variables. Composite analysis is a common way to present the responses associated with a certain climate condition by averaging the data over the considered periods. Therefore, the composite results of atmospheric and oceanic fields from extreme years will be also used to examine the relationship between the IOSD and

the IOD. The student's t-test is used to assess the statistical significance of the results obtained from statistical analyses.

3 Interannual variability of Indian Ocean SST

The purpose of this section is to analyze the variability of the oceanic surface temperatures during the 52 a period (1958–2010), by carrying out the EOF analyses on the SSTA field. The product of pattern and time series gives the actual anomaly described by the EOF. The former and the latter are often called a dominant mode and a principal component (PC), respectively. Only these products have a physical meaning. Since the results of EOF analysis are sensitive to choice of the region, we perform the EOF analysis on the monthly SSTA over the whole Indian Ocean Basin (60°S–25°N, 30°–120°E), the southern Indian Ocean (60°–10°S, 30°–120°E) and the tropical Indian Ocean (20°S–25°N, 30°–120°E), respectively.

3.1 *The primary EOF mode*

The first EOF modes in the three different regions of the whole Indian Ocean, the tropical Indian Ocean, and the southern Indian Ocean explain 28%, 45%, and 26% of the total variance, respectively. The spatial patterns are depicted in Figs 1a–c. They are labeled WM1, TM1, SM1, respectively. Figure 1d shows the corresponding temporal variability, represented by WPC1, TPC1 and SPC1.

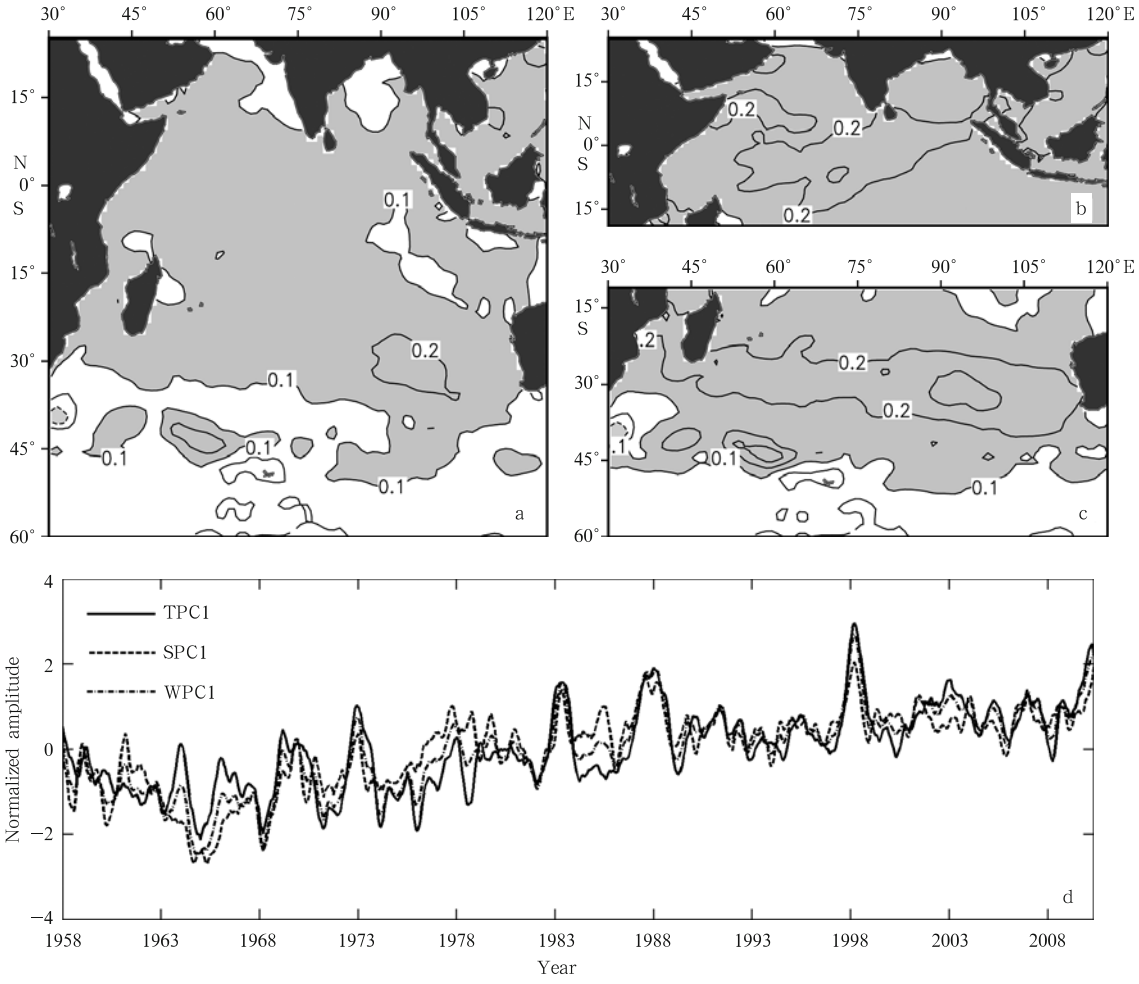

Fig.1. The space distribution of the first EOF mode associated with SSTA for the whole Indian Ocean (WM1) (a), the tropical Indian Ocean (TM1) (b), the southearn Indian Ocean (SM1) (c) and the corresponding expansion time series (d), with solid line denoting TPC1, dashed line denoting SPC1, dot-dashed line denoting WPC1.

From Fig. 1, we can see that all the first EOF modes exhibit a monopole pattern extending over the entire domain. In order to compare the similarity between WM1, TM1 and SM1, we calculate the pattern correlations between them. A pattern correlation coefficient between the tropical regions in WM1 and TM1 is as high as 0.95, far exceeding 99.9% confidence level; and that between the southern regions in WM1 and SM1 reaches 0.96. To further examine the relations between the first modes, we calculate the cross-correlation between the corresponding time expansion series. Results are shown in Table 1. The correlation coefficients between SPC1, TPC1 and WPC1 are larger than 0.9, and that between SPC1 and TPC1 also reaches 0.74, exceeding 99.9% confidence level. These spatial and temporal patterns and the correlation results suggest that the dominant modes in different domains of the Indian Ocean show the same characteristic of a basin-wide warming.

The wavelet spectral analysis of the three PCs suggests that the first EOF modes oscillate on mainly 25 a period of interdec-

Table 1. Cross-correlation coefficients between the time series of the first EOF modes of the SST variability in different regions of the whole Indian Ocean (WIO), the southern Indian Ocean (SIO) and the tropical Indian Ocean (TIO) over 1958–2010

	WPC1	SPC1	TPC1
WPC1	1.00	0.92	0.93
SPC1		1.00	0.74
TPC1			1.00

Note: Only the values significant at 99.9% confidence level are shown.

adal time scale and 3–7 a coinciding with the ENSO signal on the interannual time scale. The previous studies have proved that the basin-wide warming in the tropical Indian Ocean is related to the ENSO (e.g., Tourre and White, 1997; Chambers et al., 1999). To explore the relationship between ENSO and the basin-wide warming in the different regions of the Indian Ocean, we show in Fig. 2 the lead-lag correlation coefficients between WPC1, TPC1, SPC1 and Niño3 index. The significant correlation appears when the ENSO leads PCs, implying the influence of the ENSO on the Indian Ocean. A remarkable feature is that the correlation between TPC1 and Niño3 index is much higher than that between SPC1 and Niño3 index. This indicates that the impact of ENSO on the tropical Indian Ocean is stronger than that on the southern Indian Ocean. The relatively smaller correlation coefficients between SPC1 and Niño3 imply that ENSO forcing is just one of the factors that contribute to the basin-wide mode in the southern Indian Ocean.

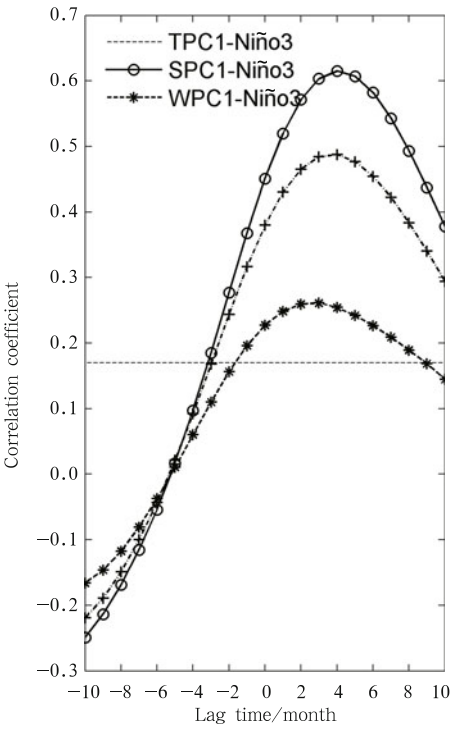

Fig.2. Lead-lag correlation coefficients between TPC1, SPC1, WPC1 and Niño3 index. PCs lag Niño3 index for positive values. Dashed line denotes 95% confidence level.

3.2 *The second EOF mode*

The second EOF modes in the three different regions of the whole Indian Ocean, the tropical Indian Ocean, and the southern Indian Ocean account for 11%, 10%, and 14% of total variance, respectively. The spatial patterns are depicted in Figs 3a–c. They are labeled WM2, TM2, SM2, respectively. The corresponding time series, represented by WPC2, TPC2 and SPC2, are shown in Fig. 4.

It is interesting that the major features of all the second EOF modes show as SSTA dipole structure. Figure 3b shows the well known IOD pattern characterized by the SSTA of opposite sign in the western and eastern tropical Indian Ocean. Following Saji et al. (1999), we use the difference between the western (TWIO: 10°N–10°S, 50°–70°E) and eastern (TEIO: 10°S–0°, 90°–110°E) SSTA as an IOD index (DMI, dashed line in Fig. 4b). This time series is related to the anomalous SST gradient across the equatorial Indian Ocean. As seen from Fig. 4b and cross-correlation results shown in Table 2, the DMI is generally consistent with TPC2.

The largest loadings appear in the subtropical region in the whole basin case (Fig. 3a). However, the IOD pattern is not present in Fig. 3a. By comparing the two dipole patterns in Figs 3a and c, we can see that they show the same structure which displays an out-of-phase relationship between temperature anomalies north and south of about 25°S in a southwest-northeast direction. The southwest and northeast centers are located at (SWIO: 40°–30°S, 50°–70°E) and (SEIO: 25°–15°S, 75°–105°E), respectively. The pattern correlation coefficient in the south Indian Ocean between WM2 and SM1 reaches 0.95. The SSTA pattern displayed here is broadly consistent with the IOSD that found by Behera and Yamagata (2001). Besides, the variabilities of WPC2 and SPC2 (Fig. 4a) are also consistent with each other, with correlation coefficient as high as 0.92 at a confidence level of 99.9% (Table 2). In addition, we have also calculated a subtropical dipole index (SDI) based on the SSTA difference between the rectangles (SWIO: 40°–30°S, 50°–70°E) and (SEIO: 25°–15°S, 75°–105°E). The two regions are similar to those suggested by Behera and Yamagata (2001). Dashed line in Fig. 4a shows the normalized (by the standard deviation) SDI thus obtained. From Fig. 4 and cross-correlation results shown in Table 2, it can be seen that the SDI generally coincides with SPC2 and WPC2. Therefore, the second EOF mode of the whole Indian Ocean SSTA is indeed dominated by the IOSD. This is further evidenced by the distribution of the standard deviation of SSTA in the Indian Ocean (Fig. 5), which shows the largest SST changes in the southern Indian Ocean, especially in the mid-latitude band where the western pole of the IOSD is located. It is instructive to look at the overlying atmospheric circulation as well. The Southern Hemisphere southeasterly trade wind stands out as particularly strong in the annual mean (figures not shown). The much great energy in the southern Indian Ocean inputted to ocean, which comes from the oscillation of atmospheric activity, contributes to the growth of oceanic variability there. In addition, there is a weak correlation between PCs/SDI and Niño3 index, which has been also mentioned in some previous literatures (Behera and Yamagata, 2001; Jia and Li, 2005; Terray and Dominiak, 2005; Feng et al., 2012).

4 Relationship between IOSD and IOD

4.1 *Correlation analysis between SPC2 and TPC2*

Positive (negative) IOD events are defined in terms of DMI exceeding one standard deviation above (below) the mean, and persisting at least for 5 months. Similarly, a positive (negative) IOSD event is defined when the value of the positive (negative)

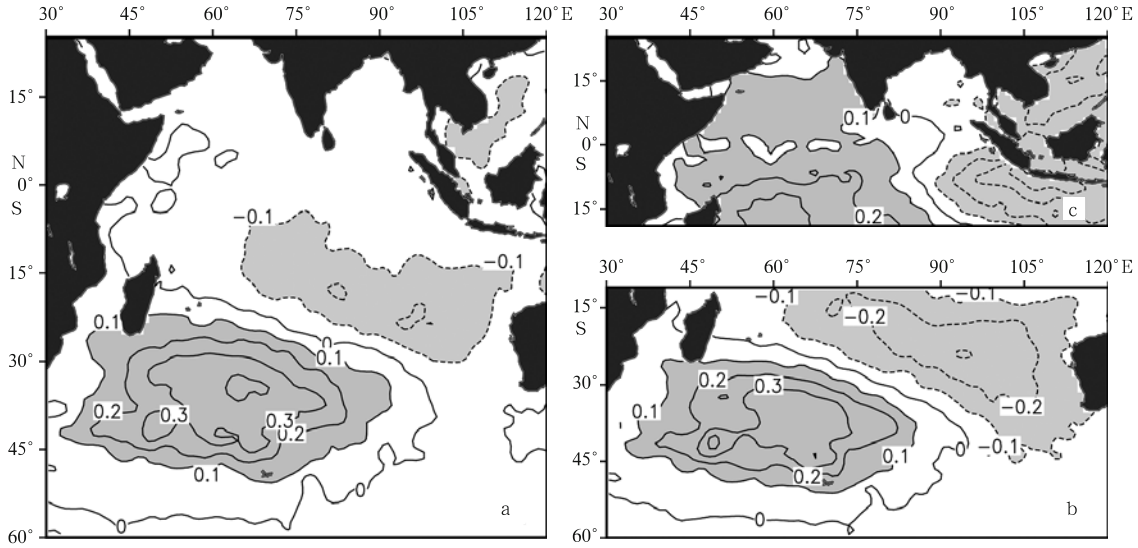

Fig.3. The space distribution of the second EOF mode associated with SSTA in the whole Indian Ocean (WM2) (a), the southern Indian Ocean (TM2) (b), and the tropical Indian Ocean (SM2) (c).

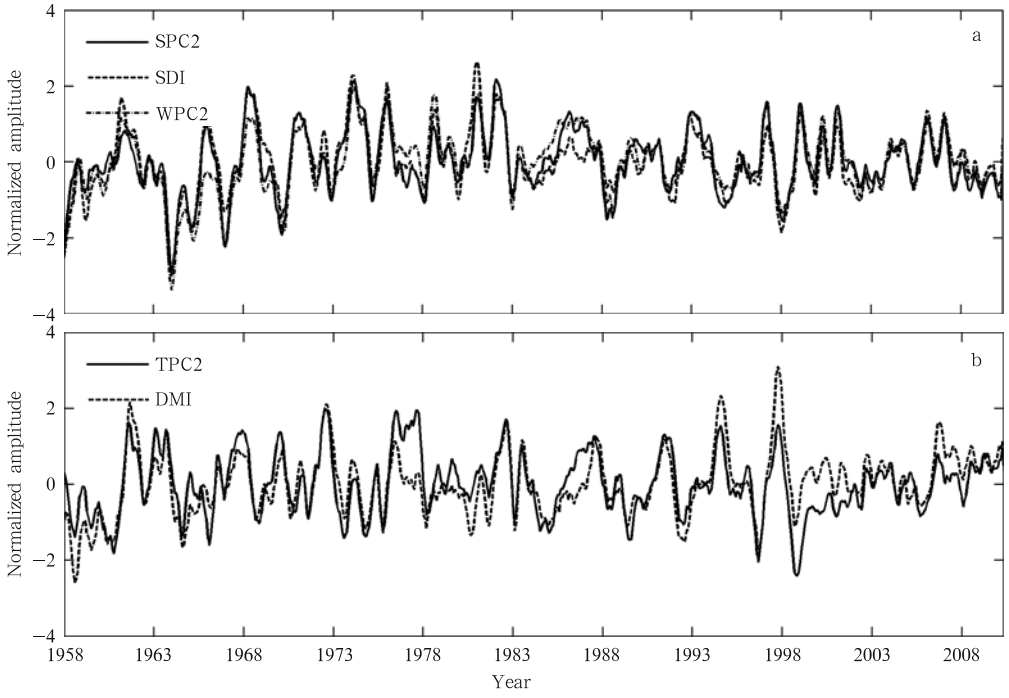

Fig.4. The associated time series of the second EOF mode shown in Fig. 3 for the whole Indian Ocean (WPC2, solide line) and the southern Indian Ocean (SPC2, dot-dashed line) (a), and the tropical Indian Ocean (TPC2, solid line) (b). Dashed lines in Figs 4a and b show the SDI and DMI, respectively.

SDI exceeds one standard deviation, and persisting at least for 5 months. To better assess the potential causal relationships between the two dipole modes in the Indian Ocean, we calculated the lead-lag correlations between SPC2 and TPC2. Results are displayed in Fig. 6. It shows that the largest correlation occurs when SPC2 leads TPC2 by about 9 months (0.59, significant at the 99% confidence level according to Student t-test), implying a potential strong forcing of the IOSD on the IOD. This result is consistent with the findings of Liu and Yu (2006). This lead-lag result indicates the important role of IOSD in the occurrence of IOD.

4.2 *Evolution of the SST variability in the Indian Ocean*

Figure 6 suggests that the Indian Ocean subtropical SST variability associated with the IOSD mode is a precursor of the SSTA dipole pattern in the tropics. In order to confirm this hypothesis, we next identify the characteristic evolutions of the SSTA in the whole Indian Ocean associated with the IOSD,

Table 2. Cross-correlation coefficients between the time series of the second EOF modes of the SST variability in different regions of the WIO (WPC2), the SIO (SPC2), the TIO (TPC2), south Indian Ocean subtropical dipole index (SDI), tropical Indian Ocean dipole index (DMI) for the 1958–2010 period

	WPC2	SPC2	TPC2
SPC2	0.92		
SDI	0.87	0.90	
DMI			0.75

Note: Only the values significant at 99.9% confidence level are shown.

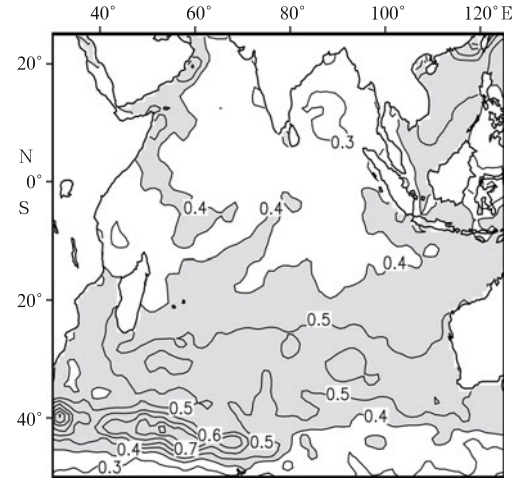

Fig.5. Standard deviation (STD) of SSTA (°C) in the Indian Ocean.

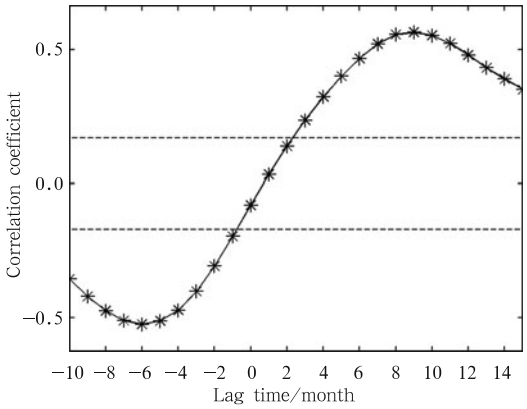

Fig.6. Lead-lag correlation between TPC2 and SPC2. TPC2 lags SPC2 for positive values. Dashed lines show 95% confidence level.

by calculating the lead-lag correlations between the SSTA and SPC2 from lags 0 up to 9 months.

By inspecting the lag correlation spatial patterns of the SSTA with SPC2, as shown in Fig. 7, it can be noted that the IOSD pattern can sustain itselves several months after its peak (i.e., at Lag +0). The negative correlations cover a large area in the eastern Indian Ocean extending southward off Australia, northward into the equatorial region. The positive correlations are found to the southeast of Madagascar. About 6 months after the peak, negative value disappears and positive value is established in the SEIO region (i.e., at Lag +6). However, the positive value in the SWIO region sustains for a longer time, till Lag +9. On the other hand, an obvious dipole structure in the tropical Indian Ocean, with positive and negative correlations in the TWIO and the TEIO, respectively, can be clearly recognized 6 months after the peak of the IOSD. It peaks at about 8–9 months lag. This time-spatial evolution of the correlation maps again indicates that if a positive (negative) IOSD event happens in the southern Indian Ocean, there may be a positive (negative) IOD event occurs in the tropical Indian Ocean, which peaks 9 months after the mature phase of the IOSD. The correlations in the tropical region shown in Fig. 7 are relatively small although they are significant. The small values imply that subtropical SST forcing associated with the IOSD is just one of the factors that contribute to interannual variations in the tropical Indian Ocean.

As we know from the lead-lag correlation analysis that the IOSD can lead to the IOD, it is possible that some of the IOD events are excited after the IOSD event. To further verify the evolutional relationship between the IOSD and IOD, we have also performed a composite analysis. As mentioned, the IOD events usually begin to develop in boreal late spring and early summer, peaking during fall, whereas the IOSD events reach a maximum in boreal winter and are phase locked to the annual cycle (e.g., Behera and Yamagata, 2001). Therefore, it is suitable to examin seasons from boreal late winter to autumn in order to identify physical fields that set the stage for the IOD occurrence. Based on the above correlation analysis, January or February seems to be a relevant starting point for the SST composite analyses. January or February SSTA will provide information on what happens, 9–10 months before the IOD events. We include all the IOSD events with mature phase in the austral summer to obtain clear composites. Identified by the SDI, we find 6 positive (1961, 1972, 1976, 1982, 2006, 2007) and 8 negative (1958, 1959, 1964, 1970, 1973, 1980, 1992, 1996) dipole events over the analysis period 1958–2010. The event year here refers to the year when the IOSD event reaches its peak in the beginning of the year. We show, in Figs 8 and 9, those composites of the SSTA for the positive and negative dipole events, respectively.

We firstly focus on examining the positive event. The time evolution of the SSTA in the entire Indian Ocean depicted in Fig. 8 is similar to the result of the lag correlation analysis shown in Fig. 7. The SSTA structure during the boreal winter has a southwest–northeast orientation in the southern Indian Ocean. The SSTA amplitude in the western pole is much larger than that in the eastern pole, which is consistent with that noted by Qian et al. (2002). This IOSD pattern maintains through boreal spring, though it decays as time progresses. The amplitude of SSTA in both poles gradually becomes smaller. Cold SSTA in the southeastern Indian Ocean has considerably weakened and the sign reveres from June, whereas the positive SWIO SSTA in the SWIO region tends to persist and slowly extends eastward.

On the other hand, in the tropical region, the cold SSTA in the eastern tropical Indian Ocean starts to develop from June. These anomalies then intensify rapidly, which is an indication that the local air-sea interactions have become active in growing the equatorial SSTA. By October-November, the IOD reaches its peak; a large-scale cooling in the eastern tropical Indian Ocean and warming in the western tropical Indian Ocean are well developed. The strongest cooling is south of equator trapped to the Sumatra-Java coast. The warm SSTA in the western tropical Indian Ocean appears on both sides of the equator

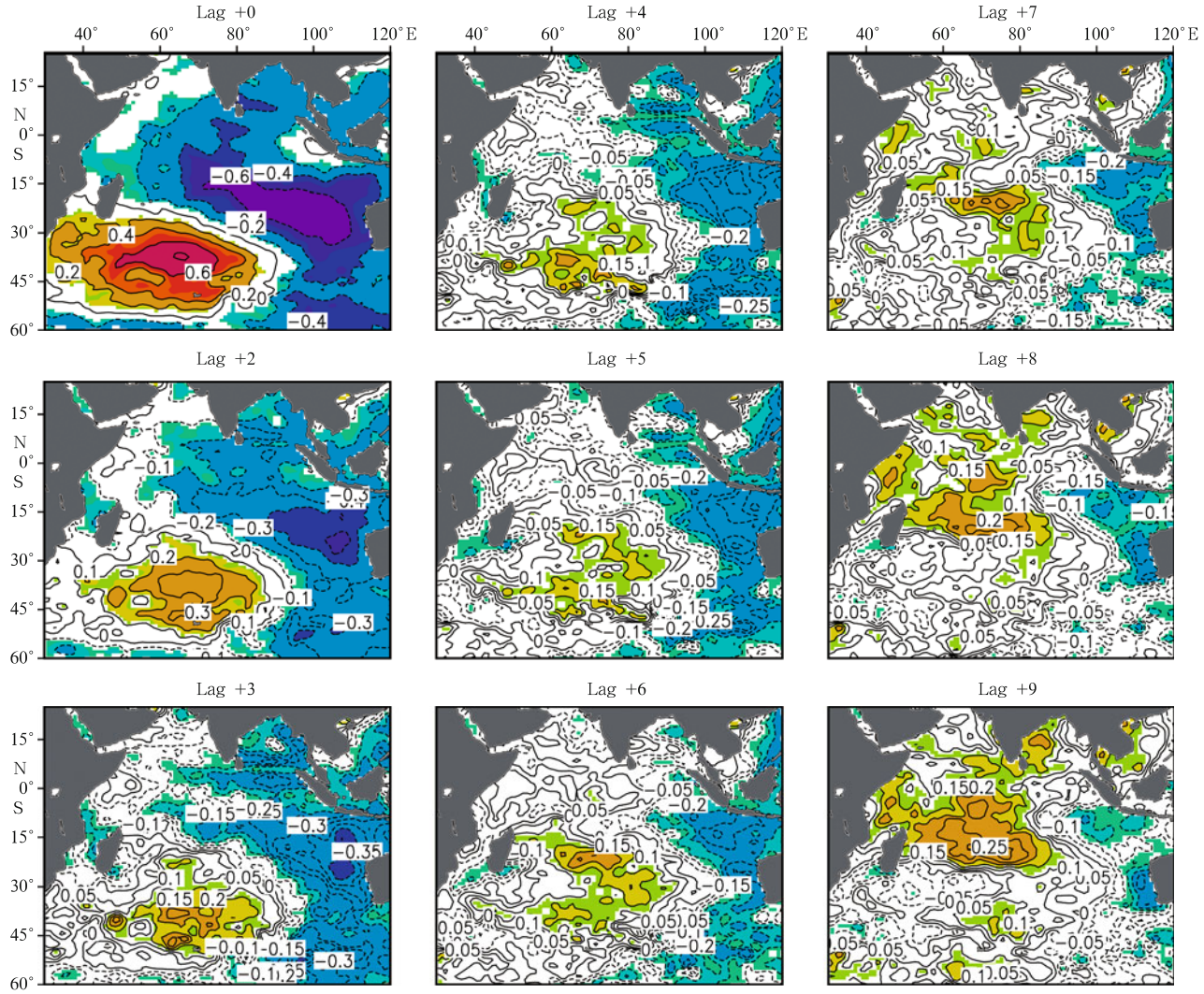

Fig.7. Lead-lag correlation maps between the SSTA and SPC2 from lag 0 months to lag 9 months. Correlation coefficients significant at the 95% confidence level according to a Student t-test are shaded. Positive lags indicate that the SPC2 leads the SSTA.

with maximum over (55°–70°E), and stretches in a northwesterly direction from the western tropical Indian Ocean toward the western side of Australia.

The reverse occurs when the negative dipole events take place. By comparing Figs 8 and 9, we can see that the composite for the negative dipole events shows a similar evolution with the positive one, except with the opposite sign. The composite study confirms a strong association of the IOD with the IOSD.

It is interesting to note that, from May on, as the season evolves, the SSTA in the SWIO starts to extend eastward, and reaches as far as 110°E by October, though the amplitude of it decays gradually, which may contribute to stretching of the IOD western pole by the mature phase in a northwest-southeast orientation (Figs 8 and 9). The feature of eastward extending of the western pole with time after the IOSD peak is also noted by Suzuki et al. (2004) from their model outputs. There is difference from our present study. The IOSD simulated by Suzuki et al. (2004) peaks in December-January, and the western pole only persists for 4 months from January to April. However, the results in this paper suggest that the SSTA in the western pole persists extending eastward for about 8–9 months from boreal late winter to early fall. In addition, different from results of Suzuki et al. (2004), in the present study, the SSTA with the negative sign in the SEIO disappears in June and is replaced by the positive value which becomes warmer and warmer thereafter.

The remarkable feature of the long persistence of the SSTA in the SWIO region associated with the IOSD presented in Figs 7–9 suggests that it may be a key factor to force the zonal SSTA dipole in the tropical Indian Ocean. In the next section, we will examine the overlying atmospheric variability to verify this hypothesis and understand the possible mechanism.

4.3 *Possible mechanisms of the IOSD triggering IOD*

To explore the possible mechanisms of the IOSD triggering IOD event, we show in Figs 10–11 the lag correlation maps of overlying atmosphere fields on the SPC2. Figure 10 displays the lag correlations between 850 hPa wind, net heat flux and SPC2, and Fig. 11 shows that of the mid-troposphere (500 hPa) vertical velocity and top-troposphere (200 hPa) wind vector.

Seen from Fig. 10, during the mature phase of the positive IOSD (i.e., at Lag +0), when the SWIO and SEIO regions are dominated by the positive and negative SSTAs, respectively, the

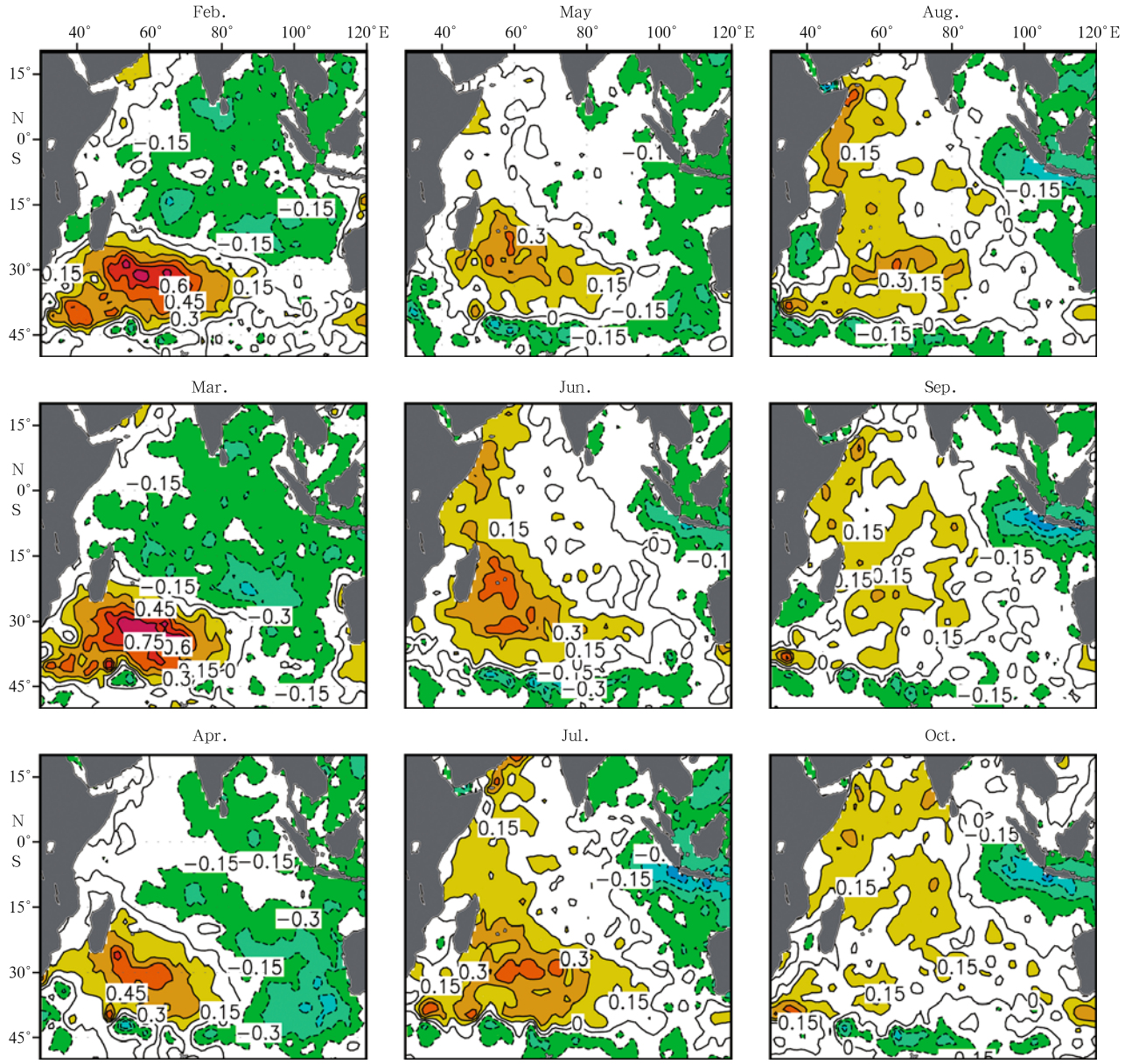

Fig.8. Monthly composites of SSTA from February to October for positive IOSD event followed by positive IOD event years over 1958–2010. Counter interval is 0.15°C. Shaded denotes values exceeds 95% confidence level.

overlying atmosphere is characterized by the intensifying of the Mascarene high. This suggests the atmosphere-to-ocean forcing.

After the peak of IOSD, over the SEIO region, northwesterly anomalies are generated under the forcing of the underlying cold SSTA (Lag +1), weakening the climatological southeasterly winds. Consequently, the weaker-than-normal wind results in smaller-than-normal ocean-to-atmosphere surface heat fluxes by reducing the latent heat flux due to a weakened evaporation. Therefore, the wind-evaporation-SST feedback mechanism of Xie and Philander (1994) is responsible for the rapidly decaying of the cold SSTA. A few months later, the positive SSTA is established (see after Lag +6). The positive net heat flux anomalies (ocean gains heat) in this region shown in Fig. 10 support this hypothesis.

Conversely on the SWIO region, as mentioned in the previous section, the positive SSTA sustains for several months after the peak of positive IOSD, with the amplitude gradually decaying. What is the possible mechanism? It can be seen from Fig. 11 that, the negative omega anomalies (anomalous ascent) are observed at 500 hPa from Lag +1 to Lag +3, indicating the increasing of the cloud cover and decreasing of the downward solar radiation there. As a result, a negative net heat flux is observed during this period (Fig. 10), favoring for the decaying of the positive SSTA. However, from Lag +4 to Lag +7, the net heat flux in the air-sea interface increases due to the decreasing of the wind speed, hindering the positive SSTA becoming smaller. It is this positive wind-evaporation-SST feedback mechanism that makes a long persistence of the positive SSTA in the SWIO. During the long period from Lag +1 to Lag +9, a

cyclonic circulation develops in the southwestern Indian Ocean around 30°S, which is expected to be generated by the underlying warm SSTA forcing (Fig. 10). This is in agreement with a linear quasi-geostrophic theory that a low pressure anomaly is generated near the warm SSTA (Terray et al., 2007). The cyclonic circulation at 850 hPa appears as response to the low pressure. We have mentioned in the previous paragraph that the positive SSTA in this region can extend eastward as time processes. The overlying anomalous cyclone driven by this SST variation also gradually spreads toward the east. It strongly weakens the subtropical Mascarene high. Consequently, the circulation over the Arabian Sea responds to the pressure difference between the Mascarene high and the monsoon trough in the tropical Indian Ocean. As a result, an anticyclone develops over Arabian Sea-India. The equatorial westerly wind in the northwestern Indian Ocean weakens after Lag +3. An anomalous easterly appears along the equatorial Indian Ocean, which is essential to the occurrence of the IOD event. Therefore, these long persistent subtropical SSTA in the western pole of the IOSD establishes the strong atmosphere circulation in the equatorial Indian Ocean to initiate the tropical SSTA, by forcing the Mascarene high. This is further evidenced by lead-lag correlations between Mascarene high index (MHI, defined as the sea level pressure averaged in the region (35°–25°S, 40°–90°E)) and SPC2, shown in Fig. 12. The positive relationship between the MHI and the SPC2 before the IOSD peaks demonstrates that the Mascarene high is one forcing factor of the IOSD, which has been mentioned in previous studies (e.g., Venegas et al., 1998; Goddard and Graham, 1999; Behera and Yamagata, 2001; Reason, 2001, 2002). However, after the mature phase of IOSD, there are significant negative correlations between MH and SPC2, MH weakens during the decaying phase of the positive IOSD. This indicates that the atmosphere responses to the underlying ocean temperature.

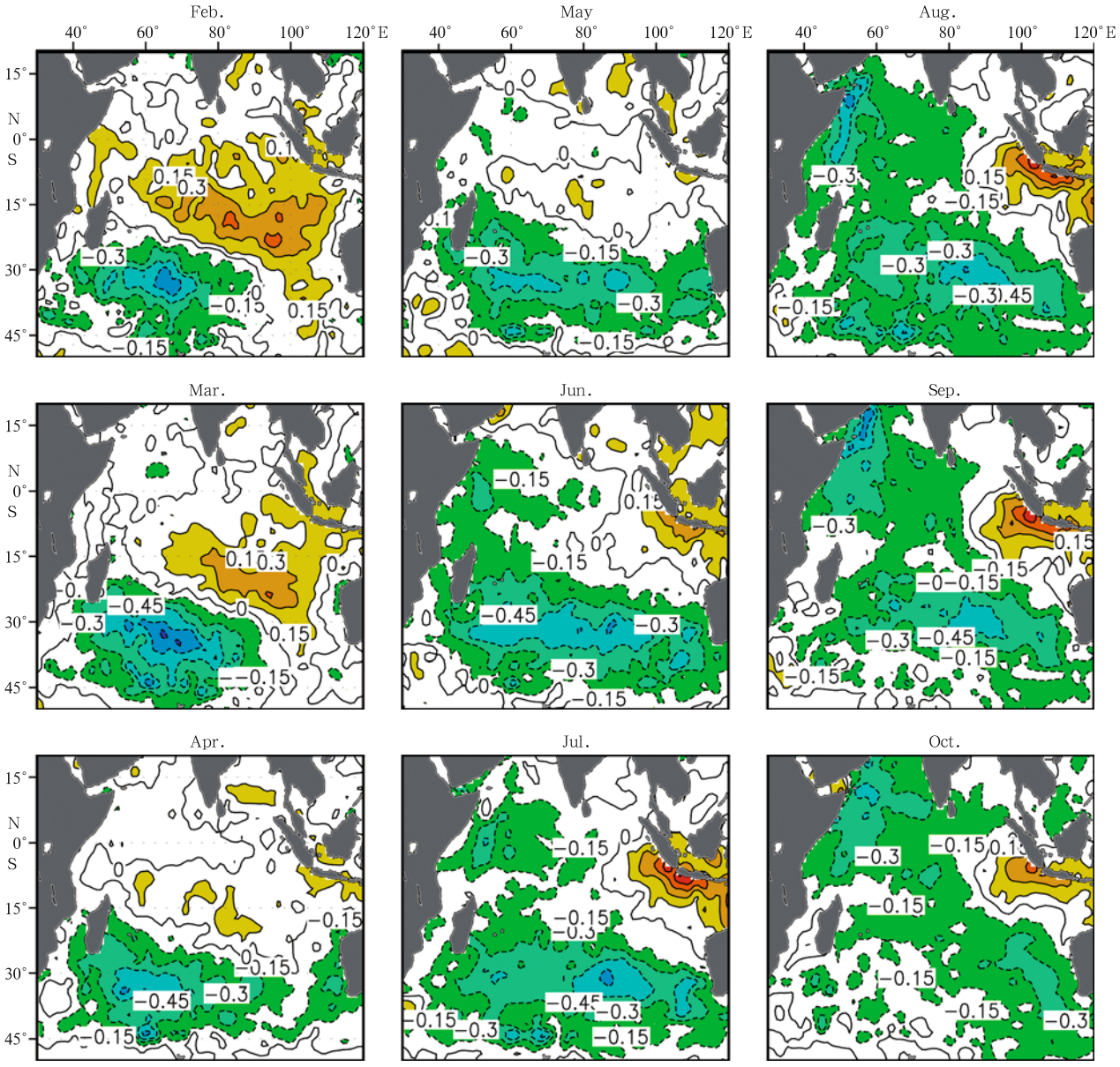

Fig.9. Same as Fig. 8, but for four negative SIOD event followed by negative IOD event years over 1958–2010.

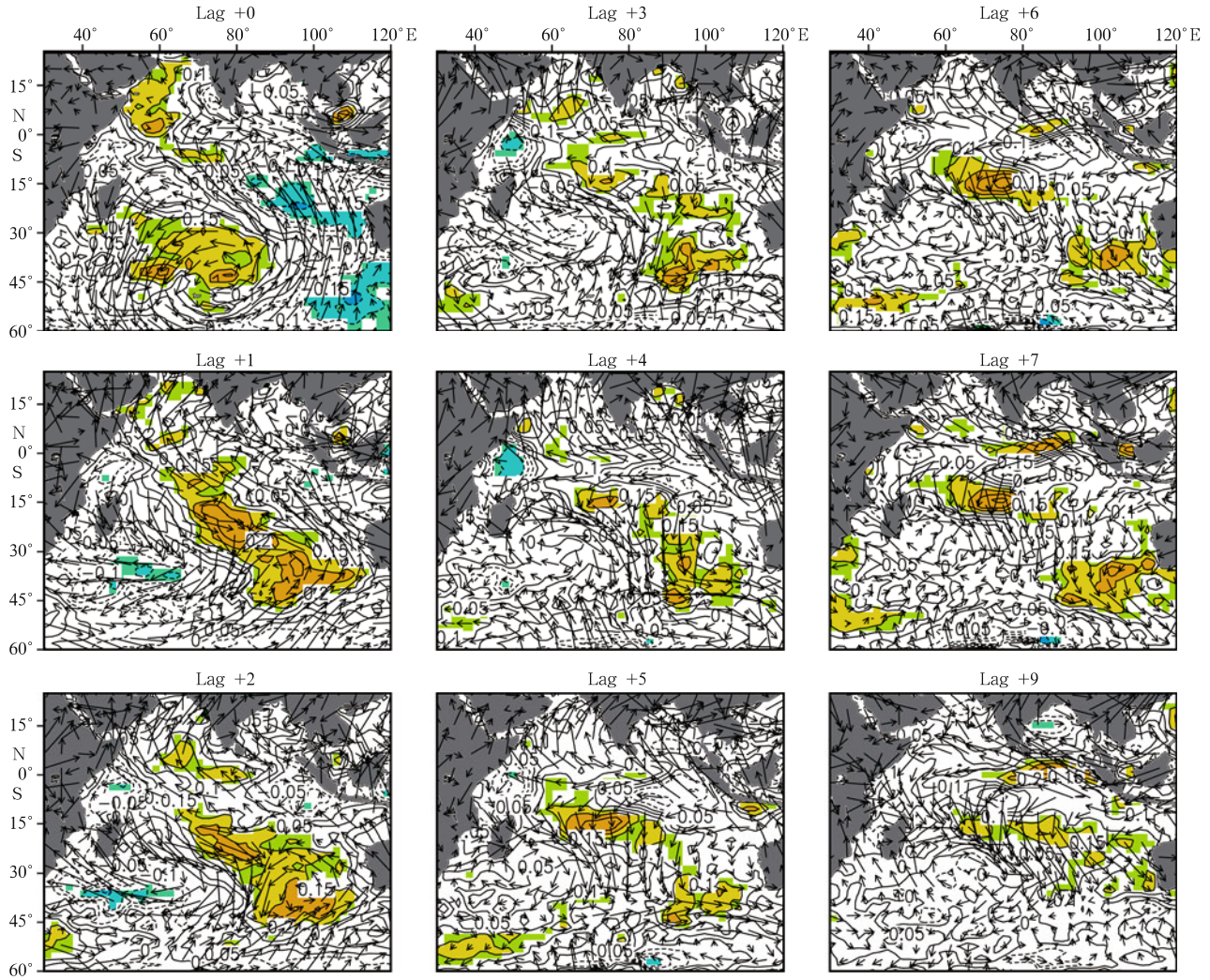

Fig.10. Lead-lag correlation maps of net heat flux anomaly (contour, positive heat flux anomaly means ocean gains heat), with shaded denoting values significant at the 95% confidence level according to a Student *t*-test, and 850 hPa wind (vector) with SPC2 from lag 0 months to lag 9 months. Positive lags indicate the SPC2 leads the net heat flux anomaly and wind.

The cooling of the eastern pole of IOD begins to develop at Lag +5 and grows in the following season (Lag +6 to Lag +9). At the same time, the high pressure appears in the mid-eastern equatorial Indian Ocean, due to the forcing of the cold SSTA. The southeasterly wind associated with this high pressure off Sumatra coast acts to intensify the background wind, because the surface mean wind in this area is southeasterly. This leads to more latent heat loss and oceanic upwelling process. As a result, the eastern tropical Indian Ocean SSTA becomes cold further under the forcing of wind-thermocline-SST feedback and the wind-evaporation-SST feedback.

Meanwhile, a zonal structure is observed along the equatorial Indian Ocean (Figs 10 and 11, from Lag +6 to Lag +9). Negative omega anomalies (anomalous ascent) are observed at 500 hPa over the western tropical Indian Ocean. At the same time, there are positive omega values (anomalous subsidence) over the eastern Indian Ocean-western Pacific. The significant easterly wind anomalies along the equatorial Indian Ocean at 850 hPa and westerly at 200 hPa are dynamically consistent with this zonal circulation. The easterlies along the equator associated with the anticyclone in the northern Indian Ocean contribute to the prominent of the tropical easterly wind. As a result, the warm water from the eastern Indian Ocean warm pool accumulates to the western Indian Ocean under the forcing of the tropical easterly winds. Again, the cold SSTA in the eastern Indian Ocean can reduce the atmospheric convection and rainfall as suggested by the significant positive omega anomalies at 500 hPa between Indo-China Peninsula and Australia (Fig. 11, Lag +6 to Lag +9). This further enhances the mean southeasterly flow off Sumatra which, in turn, reinforces the underlying cold SSTA. Thus, forced by the air-sea coupled system, the SSTA in the tropical Indian Ocean depicts the appearance of an IOD event with an anomalous SST gradient and strong easterly wind anomalies. In addition, we have calculated the composite maps of the wind field (figures not shown), which also show a similar pattern with the lag correlation results. It is well worth to emphasizing again that this IOD evolution occurs, to a great extent, associated with the positive IOSD about 9 months before.

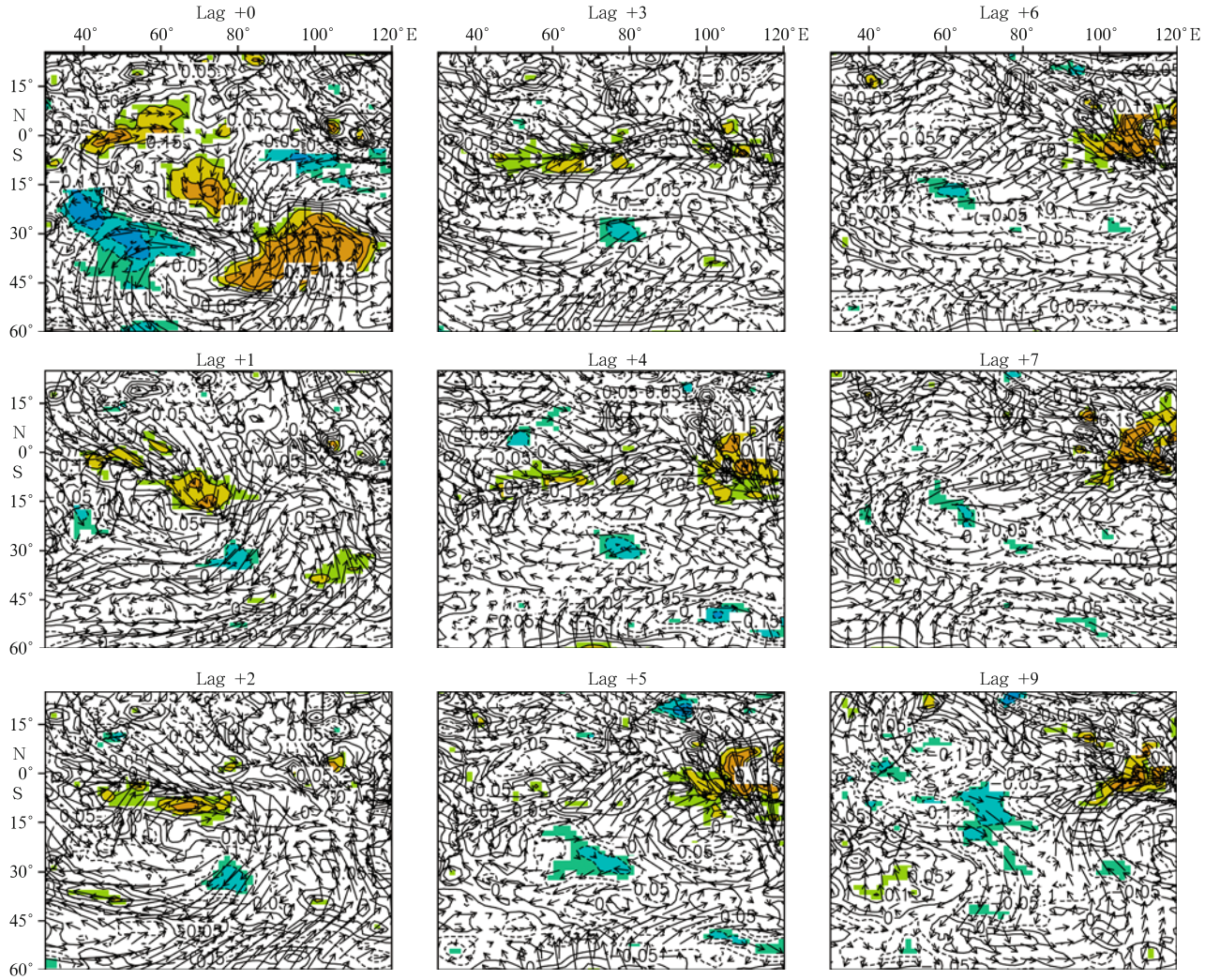

Fig.11. Lead-lag correlation maps of 500 hPa vertical velocity (contour) and 200 hPa wind (vector) with SPC2 from lag 1 months to lag 9 months. Correlation coefficients between 500 hPa vertical velocity and SPC2 significant at the 95% confidence level according to a Student t-test are shaded. Positive lags indicate the SPC2 leads the wind fields.

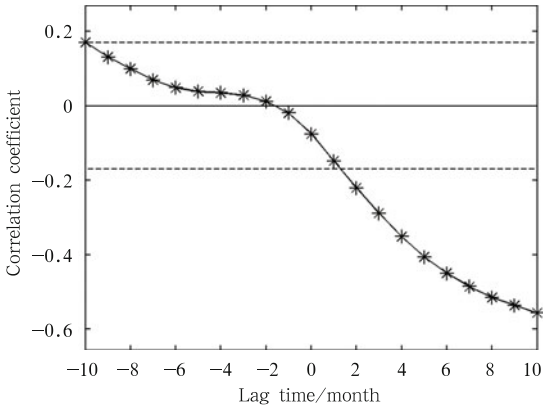

Fig.12. Lead-lag correlation between Mascarene high index (MHI) and SPC2. MHI lags SPC2 for positive values. Dashed lines show 95% confidence level.

5 Summary and conclusions

In this paper, the signals of interannual variability of the Indian Ocean in the different regions have been extracted from the monthly SST by carrying out the EOF analysis. The results suggest that the first modes are all basin modes in different regions, which are associated with the ENSO. The IOSD mode is the second mode of the SST variability both in the southern Indian Ocean and over the entire basin. However, the IOD mode only presents when the EOF analysis is conducted in the tropical region. It does not appear when the EOF analysis is applied in the whole Indian Ocean Basin. This is because the large-open southern Indian Ocean can obtain much more energy from the overlying atmosphere, which makes the oceanic variability much more active.

The lead-lag correlation analysis reveals that the IOSD event during boreal winter is one of potential forcing factor for the growth of the IOD event peaked in the following boreal fall. To clarify the physical processes of the IOSD exciting the IOD event during its decay phase, the composite fields of SSTA and lag correlations of air-sea variability on IOSD over the Indian Ocean were examined. Figure 13 shows the schematic diagrams of the possible physical process that the positive IOSD event exits the positive IOD event. The results suggest that the

SST anomalies in the western pole of the IOSD persist and slowly propagate eastward through the subsequent spring, summer and fall, providing a prolonged impact on the atmosphere circulation of the Indian Ocean. The positive wind-evaporation-SST feedback mechanism is responsible for sustaining these SST anomalies. Forced by these positive (negative) SST anomalies, the overlying Mascarene high weakens (intensifies). As a result, an anticyclone (a cyclone) develops over Arabian Sea-India, responding to the increased (decreased) pressure difference between the Mascarene high and the monsoon trough in the tropical Indian Ocean. The equatorial westerly wind in the northwestern Indian Ocean weakens (enhances) after boreal late spring. The anomalous easterly (westerly) appears along the equatorial Indian Ocean, which is essential to the occurrence of the positive (negative) IOD event. Therefore, these long persistent subtropical SST anomalies in the western pole of the IOSD establish a strong atmosphere variation in the equatorial Indian Ocean to initiate tropical SST anomalies, by forcing the Mascarene high. In one word, during the decay phase of a positive (negative) IOSD, the Mascarene high weakens (intensifies), which can then induce a positive (negative) IOD develops in tropical by exciting the equatorial easterly (westerly) wind through air-sea teleconnection. The occurrence of IOSD and IOD can be linked in sequence by the variations of Mascarene high. This is another kind of atmosphere bridge mechanism, but this bridge links the two dipole modes in the tropical and subtropical Indian Ocean.

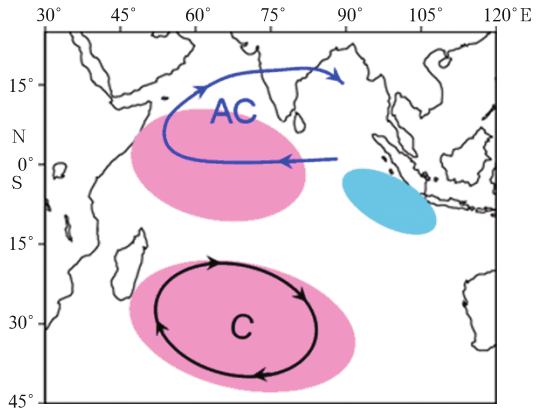

Fig.13. Schematic diagrams showing the circulation anomalies associated with the positive IOSD event that triggering the positive IOD event. Red and blue shaded areas indicate positive and negative SSTAs, respectively. Solid lines indicate the anomalous circulation at 850 hPa, and heavy arrows represent anomalous wind directions. "C" and "AC" indicate cyclonic and anticyclonic circulation anomalies, respectively.

This study shows that the IOD can be an extratropical-excited mode of the tropical Indian Ocean variability and also suggests that the decay of the IOSD can lead to the onset of IOD with the aid of atmosphere circulation. The role of the southwestern Indian Ocean SSTA during the decay phase of IOSD in triggering and reinforcing the equatorial easterly, which gives rise to the formation of IOD, is an important finding of the present study, since it implies that the SWIO SSTA associated with the IOSD event is a significant precursor of the IOD. This connection appears to be at work during 1960/1961, 1971/1972, 1975/1976, 1981/1982, 2005/2006, 2006/2007, which are all positive IOSD events and followed by positive IOD events; and during 1957/1958, 1958/1959, 1963/1964, 1969/1970, 1972/1973, 1979/1980, 1991/1992, 1995/1996, which are all negative IOSD events and followed by negative IOD events. The above result is based on the statistical analysis of observations and reanalysis data. The numerical experiments should be conducted to investigate the details of the dynamic and thermodynamic processes, especially in point of view of quantity, in the further study.

Acknowledgements

The reanalysis atmosphere dataset is from ECMWF data sever. The SST is provided by Hadley data center. We are grateful to Chen Yongli for helpful discussion and Ma Yixin for polishing the language.

References

Alexander M A, Blade I, Newman M, et al. 2002. The atmospheric bridge: the influence of ENSO teleconnections on air-sea interaction over the global oceans. J Climate, 15: 2205–2231

Annamalai H, Murtugudde R, Potemra J, et al. 2003. Coupled dynamics over the Indian Ocean: spring initiation of the zonal mode. Deep-Sea Res, 50(12): 2305–2330

Ashok K, Guan Z Y, Yamagata T. 2003. A look at the relationship between the ENSO and the Indian Ocean dipole. J Meteor Soc Japan, 81(1): 41–56

Baquero-Bernal A, Latif M, Legutke S, et al. 2002. On dipole like variability in the tropical Indian Ocean. J Climate, 15: 1358–1368

Behera S K, Luo J J, Masson S, et al. 2006. A CGCM study on the interaction between IOD and ENSO. J Climate, 19: 1688–1705

Behera S K, Yamagata T. 2001. Subtropical SST dipole events in the southern Indian Ocean. Geophys Res Lett, 28: 327–330

Bjerknes J. 1969. Atmospheric teleconnections from the equatorial Pacific. Mon Wea Rev, 97: 163–172

Cai Wenju, Hendon H, Meyers G. 2005. Indian Ocean dipole like variability in the CSIRO Mark 3 coupled climate model. J Climate, 18: 1449–1468

Chambers D P, Tapley B D, Stewart R H. 1999. Anomalous warming in the Indian Ocean coincident with El Niño. J Geophys Res, 104: 3035–3047

Feng Junqiao, Bai Xuezhi. 2010. Impacts of the tropical Pacific coupled process on the interannual variability in the Indian Ocean. J Trop Meteor, 16(3): 271–279

Feng Junqiao, Hu Dunxin, Yu Lejiang. 2012. Low-frequency coupled atmosphere-ocean variability in the southern Indian Ocean. Advances in Atmosphere Sciences, 29(3): 544–560

Feng Ming, Meyers G. 2003. Interannual variability in the tropical Indian Ocean: a two-year time scale of the Indian Ocean dipole. Deep-Sea Research, 50(12): 2263–2284

Fischer A S, Terray P, Guilyardi E, et al. 2005. Two independent triggers for the Indian Ocean dipole/zonal mode in a coupled GCM. J Climate, 18(17): 3428–3449

Goddard L, Graham N. 1999. Importance of the Indian Ocean for simulating rainfall anomalies over eastern and southern Africa. J Geophys Res, 104(D16): 19099–19116

Gordon A L. 1986. Interocean exchange of thermocline water. J Geophys Res, 91: 5037–5046

Hastenrath S, Polzin D. 2004. Dynamics of the surface wind field over the equatorial Indian Ocean. Quart J Roy Meteor Soc, 130: 503–517

Hendon H H. 2003. Indonesian rainfall variability: impact of ENSO and local air-sea interaction. J Climate, 16(11): 1775–1790

Hilary S, Rowan S, Julia S, et al. 2005. Indian Ocean climate and dipole variability in Hadley centre coupled GCMs. J Climate, 18(13): 2286–2307

Jia Xiaolong, Li Chongyin. 2005. Dipole oscillation in the southern Indian Ocean and its impacts on climate. Chin J Geophys (in Chinese), 48(6): 1238–1249

Kalnay E, Kanamitsu M, Kistler R, et al. 1996. The NCEP/NCAR 40-year reanalysis project. Bull Amer Meteor Soc, 77: 437–470

Klein S A, Soden B J, Lau N C. 1999. Remote sea surface temperature variations during ENSO: evidence for a tropical atmospheric bridge. J Climate, 12: 917–932

Latif M, Barnett T P. 1995. Interactions of the tropical oceans. J Climate, 8(4): 952–964

Lau N C, Nath M J. 2000. Impact of ENSO on the variability of the Asian-Australian monsoons as simulated in GCM experiments. J Climate, 13: 4287–4309

Lau N C, Nath M J. 2003. Atmosphere-ocean variations in the Indo-Pacific sector during ENSO episodes. J Climate, 16: 3–20

Li Tim, Wang Bin, Chang C, et al. 2003. A theory for the Indian Ocean dipole-zonal mode. J Atmos Sci, 60(17): 2119–2135

Liu Yun, Feng Ming, Church John, et al. 2005. Effect of salinity on estimating geostrophic transport of the Indonesian throughflow along the IX1 XBT section. J Oceanogr, 61(4): 795–801

Liu Qinyan, Huang Ruixin, Wang Dongxiao. 2012. Implication of the South China Sea throughflow for the interannual variability of the regional upper-ocean heat content. Adv Atmos Sci, 29(1): 54–62

Liu Qinyan, Wang Dongxiao, Zhou Wen, et al. 2010. Covariation of the Indonesian throughflow and South China Sea throughflow associated with the 1976/77 regime shift. Adv Atmos Sci, 27(1): 87–94

Liu Lin, Yu Weidong. 2006. Connection between tropical Indian Ocean dipole event and subtropical Indian Ocean dipole event. Advances in Marine Science (in Chinese), 24(3): 301–306

Qian Weihong, Hu Haoran, Deng Yi, et al. 2002. Signals of interannual and interdecadal variability of air-sea interaction in the basin-wide Indian Ocean. Atmos Ocean, 40: 293–311

Rao S A, Behera S K, Masumoto Y, et al. 2002. Interannual variability in the subsurface Indian Ocean with special emphasis on the Indian Ocean dipole. Deep-Sea Res Pt II, 49: 1549–1572

Reason C J. 2001. Subtropical Indian Ocean SST dipole events and southern African rainfall. Geophys Res Lett, 28: 2225–2227

Reason C J. 2002. Sensitivity of the southern African circulation to dipole sea-surface temperature patterns in the south Indian Ocean. Int J Climatol, 22: 377–393

Saji N H, Goswami B N, Vinayachandran P N, et al. 1999. A dipole mode in the tropical Indian Ocean. Nature, 401: 360–363

Shinoda T, Hendon H H, Alexander M A. 2004. Surface and subsurface dipole variability in the Indian Ocean and its relation with ENSO. Deep-Sea Res, 51(5): 619–635

Subrahmanyam M V, Wang Dongxiao. 2011. Impact of latent heat flux on Indian summer monsoon during El Niño/La Niña years. J Trop Meteor, 17(4): 430–440

Suzuki R, Behera S K, Iizuka S, et al. 2004. Indian Ocean subtropical dipole simulated using a coupled general circulation model. J Geophys Res, 109: C09001, doi:10.1029/2003JC001974

Terray P, Dominiak S. 2005. Indian Ocean sea surface temperature and El Niño-Southern Oscillation: a new perspective. J Climate, 18: 1351–1368

Terray P, Fabrice C, Herve D. 2007. Impact of southeast Indian Ocean sea surface temperature anomalies on monsoon-ENSO-dipole variability. Clim Dyn, 28: 553–580

Tourre Y M, White W B. 1997. Evolution of the ENSO signal over the Indo-Pacific domain. J Phys Oceanogr, 27: 683–696

Venegas S A, Mysak L A, Straub D N. 1998. An interdecadal climate cycle in the South Atlantic and its links to other ocean basins. J Geophys Res, 103: 24723–24736

Wang Dongxiao, Liu Qinyan, Liu Yun, et al. 2004. Connection between interannual variability of the western Pacific and eastern Indian Oceans in the 1997–1998 El Niño event. Progress in Natural Science, 14(5): 423–429

Wang Dongxiao, Wu Guoxiong, Xu Jianjun. 1999. Interdecadal variability in the tropical Indian Ocean and its dynamic explanation. Chinese Science Bulletin, 44(17): 1620–1627

Webster P J, Magana V O, Palmer T N, et al. 1998. Monsoons: processes, predictability and the prospects for prediction. J Geophys Res, 103(C7): 14451–14510

Webster P J, Moore A M, Loschnigg J P, et al. 1999. Coupled ocean-atmosphere dynamics in the Indian Ocean during 1997-98. Nature, 401(6751): 356–360

Wu Bo, Li Tim, Zhou Tianjun. 2010. Relative contributions of the Indian Ocean and local SST anomalies to the maintenance of the western North Pacific anomalous anticyclone during El Niño decaying summer. J Climate, 23: 2974–2986

Wu Bo, Zhou Tianjun, Li Tim. 2009. Seasonally evolving dominant interannual variability modes of East Asian climate. J Climate, 22: 2992–3005

Wu Bo, Zhou Tianjun, Li Tim. 2011. Two distinct modes of tropical Indian Ocean precipitation in boreal winter and their impacts on equatorial western Pacific. J Climate, 25(3): 921–938

Xie Shangping, Annamalai H, Schott F A, et al. 2002. Structure and mechanisms of south Indian Ocean climate variability. J Climate, 15: 864–878

Xie Shangping, Philander S G H. 1994. A coupled ocean-atmosphere model of relevance to the ITCZ in the eastern Pacific. Tellus, 46A: 340–350

Yu Jinyi, Lau K M. 2004. Contrasting Indian Ocean SST variability with and without ENSO influence: a coupled atmosphere-ocean GCM study. Meteor Atmos Phys, 90, doi: 10.1007 /s00703-004-0094-7

Zhao Yongping, Chen Yongli, Wang Fan, et al. 2009. Two modes of dipole events in tropical Indian Ocean. Sci China: Ser D-Earth Sci, 52(3): 369–381

Zhou Tianjun, Wu Bo, Wang Bin. 2009. How well do atmospheric general circulation models capture the leading modes of the interannual variability of the Asian-Australian monsoon? J Climate, 22: 1159–1173